Chapter 1
An instability result for suspension bridges

C. Marchionna and S. Panizzi

Abstract We consider a class of second order systems of two ODEs which arise as single mode Galerkin projections of the so-called fish-bone [BG] model of suspension bridges. The two unknowns represent flexural and torsional modes of vibration of the deck of the bridge. The nonlinear elastic responses $\mathscr{F}$ of the cables are supposed to be generalizations of the slackening regime. In the first part, under the assumption of sub-linear growth for $\mathscr{F}$ we establish a condition depending on a set of 3 parameters under which the flexural motions are unstable provided the energy is sufficiently large. In the last part of the paper we numerically investigate the effect of slackening for different model functions, either sub-linear or super-linear. Finally, we examine the different types of bifurcations that give rise to instability of flexural modes.

1.1 Introduction

An important issue in the mathematical modeling of suspension bridges is the phenomenon of energy transfer from flexural to torsional modes of vibration along the deck of the bridge. The sudden change from a vertical to a torsional mode of oscillation can be dramatically destructive, see for example the collapse of the Tacoma Narrows Bridge.

The purpose of our results is to provide a contribution to a recent field of research beginning from [AG], [BG], and summarized in [Gaz], according to which internal

C. Marchionna
Dipartimento di Matematica, Politecnico di Milano, Milano, ITALY
e-mail: clelia.marchionna@polimi.it

Stefano Panizzi
Dipartimento di Matematica e Informatica, Universitá degli Studi di Parma, Parma, ITALY,
e-mail: stefano.panizzi@unipr.it

nonlinear resonances giving rise to the onset of instability may occur even when the aeroelastic coupling is disregarded.

The suspension bridge model (*fish-bone* model) under consideration has been proposed by K.S. Moore [Moo], revisited and somehow simplified in [BG]. The dynamics of the midline of the deck, modeled as an Euler-Bernoulli beam of length L and width $2l$, is coupled with the elastic response of the suspension cables acting on the side ends of the deck. The cross section of the deck is assumed to be a rigid rod with mass density ρ, length $2l$ and negligible thickness with respect to l; $y(x,t)$ is the vertical downward deflection of the midline of the deck with respect to the unloaded state, $\theta(x,t)$ is the angle of rotation of the deck with respect to the horizontal position.

The corresponding PDEs system is

$$\begin{cases} \rho S y_{tt} + EI\, y_{xxxx} + \mathscr{F}(y + l\sin\theta) + \mathscr{F}(y - l\sin\theta) = 0 \\ \rho J\, \theta_{tt} - GJ\theta_{xx} + l\cos\theta\,[\mathscr{F}(y + l\sin\theta) - \mathscr{F}(y - l\sin\theta)] = 0 \end{cases}$$

with hinged boundary conditions:

$$y(0,t) = y(L,t) = y_{xx}(0,t) = y_{xx}(L,t) = 0, \quad \theta(0,t) = \theta(L,t) = 0.$$

About the meaning of the constant parameters not yet defined: S is the cross section area, I is the planar second moment of area with respect to the plane $y = 0$, J is the polar second moment of area with respect to the x-axis and E and G are respectively Young's modulus and the shear modulus.

The restoring force $\mathscr{F}$ exerted by the hangers is applied to both extremities of the deck whose displacements from the unloaded state are given by $y \pm l\sin\theta$. No external forces, except gravity, are taken in account.

In the classical slackening regime, the hangers behave as linear springs of elastic constant $\mathrm{k} > 0$ if stretched and do not exert restoring force if compressed. In this case an analytical expression of $\mathscr{F}$ is readily written as follows (see [MCKW], [Moo]):

$$\mathscr{F}(r) = \mathrm{k}\left[(r + r_0)^+ - r_0\right], \quad r_0 = \rho S g/2\mathrm{k}, \quad g \text{ is the gravity.} \tag{1.1}$$

In this note we consider several generalizations of the slackening regime (assumption (S) below), either for restoring forces having sub-linear growth at infinity or for super-linear growth, such as the forces considered in [MCKT].

Since our results aim to describe the onset of torsional instability, we neglect the behavior of the bridge when the torsional angle becomes large, and assume that, at least at the beginning, $\sin\theta \sim \theta$ and $\cos\theta \sim 1$. Setting $z = l\theta$, the PDEs system simplifies to:

$$\begin{cases} \rho S y_{tt} + EI\, y_{xxxx} + \mathscr{F}(y + z) + \mathscr{F}(y - z) = 0, \\ \rho J z_{tt} - GJ z_{xx} + \rho S l^2\, (\mathscr{F}(y + z) - \mathscr{F}(y - z)) = 0 \end{cases} \tag{1.2}$$

As a first investigation, through a Galerkin projection, we study the interaction between both the first flexural and torsional modes of vibration. Let us assume that the displacements are well approximated by their first mode of vibration, that is:

$$y(x,t) \simeq y_1(t)\sin x, \quad z(x,t) \simeq z_1(t)\sin x,$$

then, dropping the index 1, we reduce the PDEs system to the following ODEs system:

$$\begin{cases} \ddot{y}(t) + \alpha y(t) + f(y(t)+z(t)) + f(y(t)-z(t)) = 0 \\ \ddot{z}(t) + \beta z(t) + \gamma[f(y(t)+z(t)) - f(y(t)-z(t))] = 0 \end{cases} \tag{1.3}$$

with "structural parameters"

$$\alpha = \frac{EI\pi^4}{\rho SL^4}, \quad \beta = \frac{G\pi^2}{\rho L^2}, \quad \gamma = \frac{Sl^2}{J}, \tag{1.4}$$

and

$$f(r) = \frac{1}{\rho S}\frac{2}{\pi}\int_0^\pi \mathscr{F}(r\sin x)\sin x\,dx.$$

It is worth noting that the transform $\mathscr{F} \mapsto f$ falls within the family of Abel transforms, and has a slightly regularizing effect. Moreover f inherits the essential properties of $\mathscr{F}$.

The system (1.3) is conservative with an energy that, at least for the cases here considered, is nonnegative ($F(r) = \int_0^r f(s)\,ds$):

$$\mathscr{E}(y,\dot{y},z,\dot{z}) = \frac{\dot{y}^2}{2} + \frac{\dot{z}^2}{2\gamma} + \frac{\alpha}{2}y^2 + \frac{\beta}{2\gamma}z^2 + F(y+z) + F(y-z),$$

therefore all its solutions are bounded and globally defined.

We are interested in stability/instability properties of pure flexural periodic solutions of (1.3), that is solutions $(w(t),0)$, where $w(t)$ solves

$$\ddot{w}(t) + \alpha w(t) + 2f(w(t)) = 0.$$

We always assume that f satisfies the following generalization of the slackening regime.

Assumption **(S)**:

a) *f is an increasing, continuous function such that $f(0) = 0$;*

b) *f is piecewise C^1: its derivative is continuous with the exception of a finite (eventually empty) set of points $r_1 < r_2 < \ldots < r_n$ not including zero in which there exist the finite limits:*

$$\lim_{r \to r_i^{\pm}} f'(r);$$

c) *$f'(0) = m > 0$;*

d) *f has asymptotically null slope as $r \to -\infty$, i.e. $\lim_{r\to-\infty} f'(r) = 0$.*

In the first part of the paper we present some analytical results for a class of functions f with the same essential properties of the classical slackening regime (1.1), which is a finite limit slope as the displacements at the side edges of the deck $y \pm z$ get large (see also, for proofs and details [MP]). We set a condition on the parameters (1.4) and the slope M of f at $+\infty$ that guarantees instability for the pure flexural solutions, provided the energy is large enough.

Theorem 1. *Assume that f statisfies*

$$\lim_{r \to +\infty} f'(r) = M > 0, \tag{1.5}$$

in addition to assumption (S). Let us set

$$\phi_0 := \sqrt{\frac{\beta + 2\gamma M}{\alpha + 2M}}\,\pi, \qquad \phi_1 := \sqrt{\frac{\beta}{\alpha}}\,\pi, \qquad q = \sqrt{\frac{\beta + 2\gamma M}{\beta}}.$$

If

$$\Delta = \left| \cos\phi_0 \cos\phi_1 - \frac{q + q^{-1}}{2} \sin\phi_0 \sin\phi_1 \right| > 1,$$

then there exists an energy level $\mathscr{E}_0$ such that, if $\mathscr{E}(w(0), \dot{w}(0), 0, 0) > \mathscr{E}_0$, the pure flexural periodic solution $(w(t), 0)$ is unstable.

The last part of this paper shows some numerical experiments in order to compare different models of slackening satisfying the assumptions of Theorem 1 or merely satisfying **(S)** with a super-linear behavior at $+\infty$, and showing what can happen for "medium level" energy.

1.2 The isoenergetic Poincaré Map and the asymptotic behavior of its linearization $\mathscr{L}_k$

In order to prove Theorem 1, we introduce the Poincaré map at a fixed level of energy to reduce by 1 the degrees of freedom, as in [CW], and to study the asymptotic behavior of its linearization when the energy tends to infinity. Then the idea, borrowed from [CW], is that of studying the linearized system as the energy $\mathscr{E} \to \infty$ (see also [GG]). The asymptotic system happens to be less regular, but much simpler!

Let $w_k(t)$ be the solution of the Duffing equation

$$\ddot{w}_k(t) + \alpha w_k(t) + 2f(w_k(t)) = 0, \qquad w_k(0) = k > 0, \quad \dot{w}_k(0) = 0. \tag{1.6}$$

Under assumption **(S)**, $w_k(t)$ is an even periodic function, with a certain period τ_k and energy $\mathscr{E}_k$. Let us denote by $\Gamma_k = \{(w_k(t), \dot{w}_k(t), 0, 0) : t \in \mathbf{R}\}$, the orbit in the 4-dimensional phase space of $(w_k, 0)$.

In short, the isoenergetic first return Poincaré map $\mathscr{P}_k$ around Γ_k is defined as follows: Let (y, z) be a solution with the same energy of $(w_k, 0)$, with

$$y(0) > 0, \quad \dot{y}(0) = 0, \quad z(0) = z_0, \quad \dot{z}(0) = z_1$$

and let $T(z_0, z_1)$ be the first return time (which exists under some smallness assumptions on (z_0, z_1)) when the solution (y,z) crosses the section $\{\dot{y} = 0, \quad y > 0\}$, then

$$\mathscr{P}_k(z_0, z_1) = (z(T(z_0, z_1)), \dot{z}(T(z_0, z_1))).$$

We linearize the second equation of the ODEs system (1.3) around Γ_k and obtain the following Hill equation::

$$\ddot{u}(t) + \left(\beta + 2\gamma f'(w_k(t))\right) u(t) = 0 \qquad u(0) = a, \quad \dot{u}(0) = b \tag{1.7}$$

The linearized Poincaré map $\mathscr{L}_k = D\mathscr{P}_k(0,0)$ is given by $\mathscr{L}_k(a,b) = (u(\tau_k), \dot{u}(\tau_k))$, where τ_k is the period of $w_k(t)$. It is the monodromy matrix of the Hill equation, that is

$$\mathscr{L}_k = \begin{pmatrix} u^0(\tau_k) & u^1(\tau_k) \\ \dot{u}^0(\tau_k) & \dot{u}^1(\tau_k) \end{pmatrix}. \tag{1.8}$$

where $u^0(t)$ and $u^1(t)$ are the two solutions of (1.7) corresponding to the initial conditions $(1,0)$ e $(0,1)$ respectively. The periodic orbit Γ_k is unstable, if the origin is an unstable fixed point of the map $\mathscr{L}_k$.

Proposition 1. *If $\frac{1}{2}|u^0(\tau_k) + \dot{u}^1(\tau_k)| > 1$, $\mathscr{L}_k$ has two real eigenvalues λ_1, λ_2, such that $|\lambda_1| > 1$, $\lambda_2 = 1/\lambda_1$. Then the periodic orbit Γ_k is unstable.*

If in addition the periodic term of the equation (1.7) is even, the instability test simplifies as $|u^0(\tau_k)| > 1$.

In order to study the asymptotic behavior of $\mathscr{L}_k$, we normalize the solution of the Duffing equation (1.6) by setting $W_k(t) = w_k(t)/k$. The linearized system becomes

$$\begin{cases} \ddot{W}_k(t) + \alpha W_k(t) + 2\dfrac{f(kW_k(t))}{k} = 0, & W_k(0) = 1, \quad \dot{W}_k(0) = 0 \\ \ddot{u}_k(t) + (\beta + 2\gamma f'(kW_k(t)))\, u_k(t) = 0 & u_k(0) = a, \quad \dot{u}_k(0) = b \end{cases}$$

and its limit system, as $k \to \infty$ is

$$\begin{cases} \ddot{W}(t) + \alpha W(t) + 2g(W(t)) = 0, & W(0) = 1, \quad \dot{W}(0) = 0 \\ \ddot{v}(t) + (\beta + 2\gamma g'(W(t)))\, v(t) = 0, & v(0) = a, \quad \dot{v}(0) = b \end{cases}$$

where $\quad g(r) = Mr^+$.

We can prove that

- $W_k(t) \to W(t)$ in $C^2(\mathbf{R})$
- $\tau_k \to \tau_\infty \qquad (\ \tau_k, \quad \tau_\infty$ periods of W_k, $W)$,
- $u_k(t) \to v(t)$ in $C^1([0,T])$

In particular, if $u_k^0(t)$ and $v^0(t)$ are the solutions of the Hill equations with data $(1,0)$ respectively of the k-system and the limit system, then

$$u_k^0(\tau_k) \to v^0(\tau_\infty).$$

Now we begin to see where the discriminant Δ in Theorem 1 comes from: ought to the simplicity of $g(r)$, it is possible to compute $v^0(\tau_\infty) = \Delta$. If $|v^0(\tau_\infty)| > 1$, the trivial solution of the limit- Hill equation is unstable, and the same happens for the k-Hill equation, for k large enough.

Unfortunately, the method does not give any estimate on the size of the critical energy level $\mathscr{E}_0$, where this "high energy type" of instability begins to occur.

1.3 Some related problems and questions

We decided to numerically compare a set of 6 functions f in (1.3) modelling the slackening regime, all satisfying the assumption **(S)**. In order to have the same elastic response for small displacement and approximately the same level for the slackening, we chose to fix two parameters

$$f'(0) = m, \quad \lim_{r\to-\infty} f(r) = -h, \quad m,h > 0. \tag{1.9}$$

The first three functions satisfy the assumption (1.5) with the same slope $M = m = f'(0)$ at $+\infty$, as well as f_4 but with a different $M = 2m$ slope at $+\infty$. The last two functions do not meet the last condition (1.5) having polynomial and exponential growth at $+\infty$ respectively (an exponential growth was proposed by [MCKT]).

If we define the slackening point as $r_0 = h/m$, the chosen model functions are

$$f_1(r) = mr, \quad r \geq -r_0, \quad f_1(r) = -h, \quad r \leq -r_0,$$
$$f_2(r) = \int_0^{\pi/2} f_1(\frac{4}{\pi} r \sin x)\, \sin x\, dx$$
$$f_3(r) = mr, \quad r \geq 0, \quad f_3(r) = \frac{hr}{\sqrt{r^2 + r_0^2}} \quad r < 0$$
$$f_4(r) = mr + m\sqrt{r^2 + r_0^2} - h$$
$$f_{5,n}(r) = h(1 + r/(nr_0))^n - h, \quad r \geq -r_0, \quad f_{5,n}(r) = -h, \quad r \leq -r_0, \quad (n > 1)$$
$$f_6(r) = h(e^{r/r_0} - 1).$$

The first function f_1 is basically the Moore-McKenna $\mathscr{F}(r)$ in (1.1), and is so simple that allows to explicitly compute, depending on the datum $w(0) = k$, the solutions of the linearized problem defined by (1.6) and (1.7), and its instability discriminant. These analytical results have been useful to validate the Matlab numerical results for the whole set of functions. The second function f_2 is a rescaling of $\tilde{f}$ in [MP] (which we refer to for its analytical formula); precisely $f_2(r) = \frac{\pi}{4}\tilde{f}(\frac{4}{\pi}r)$, where

$\tilde{f}$ is the projection on the first eigenmode of (1.1). The function f_3 was introduced by [BFG] and is slightly more regular being $C^2(\mathbf{R})$.

From a modeling point of view, if we suppose that for larger downward deflection the stiffness has to increase, the last three function may be more suitable, with stronger stiffness behavior from f_4 to f_6.

A first mathematical remark is that the $\lim_{k\to 0} u^0(\tau_k)$ depends only on the "structural constants" (1.4) and $f'(0) = m$. More precisely, we have

$$\lim_{k\to 0} \tau_k = \frac{2\pi}{\sqrt{\alpha+2m}}, \quad \lim_{k\to 0} u^0(\tau_k) = \cos\left(\frac{2\pi\sqrt{\beta+2\gamma m}}{\sqrt{\alpha+2m}}\right).$$

So the following proposition holds, due to a continuity argument:

Proposition 2. *If $f'(0) = m$ and $\frac{2\sqrt{\beta+2\gamma m}}{\sqrt{\alpha+2m}} \notin \mathbf{N}$ then there exists a suitable level of energy $\mathscr{E}_0$ such that for lesser energies the linearized Poincaré map is stable.*

That is, if we fix, for example, α, β, and γ, we have linear stability with the exception of a countable set of values of m. A reasonable conjecture could be that the Poincaré map is stable, or at least lineary stable for every set of parameters, at suitable low energies, for all functions satisfying the **(S)** assumption. A very interesting result could be to set some upper bound for the energy in order to guarantee at least linear stability.

1.4 Numerical Examples

The following numerical simulations report the behavior of L, half the trace of the monodromy matrix of the Hill equation (1.7), as a function of $w_k(0) = k$, for the whole set of functions. In the case when $|L| < 1$ the eigenvalues of $\mathscr{L}_k$ are unitary conjugate complex numbers, and the origin is an elliptic point of the Poincaré map.

In the first example Fig.1.1, the parameters are fixed to $\alpha = \beta = 0.1$, $\gamma = 3$, $m = h = 1$. The asymptotic value of Δ is approximately $= -0.5988$, thus the map is linearly stable for high energies at least for the first four functions.

We can note that the the first interval of instability starts approximately at the same level $k = 1$, that is the value of the slackening point $r = r_0$ for all 6 sample functions, while the second instability takes place in a range $5 < k < 5.3$ for the first three sample functions. The second interval is anticipated to $k \simeq 3.6$ for the fourth function which has slope $2m$ at infinity), and no other instability arises for the last two. We can note also that the behavior of the discriminant L is smoothed out as the functions f_i gain regularity.

In our second example Fig.1.2, the parameters are fixed to $\alpha = 0.1$, $\beta = 4$, $\gamma = 3$, $m = 1$, $h = 2$. Again Theorem 1 tells us that the map is linearly stable for high energies at least for the first four functions. The effect of slackening is clear in every case at $k = 2 = r_0$, even though it is a little anticipated for f_4 and f_6. We can see

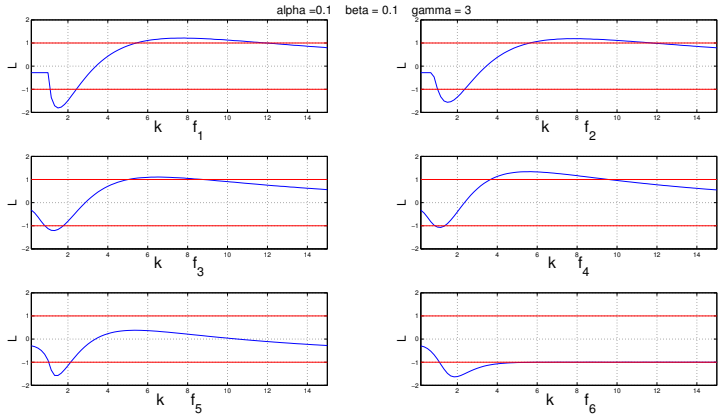

Fig. 1.1 Half the trace of the monodromy vs k. $\alpha = \beta = 0.1$, $\gamma = 3$, $m = h = 1$, $n = 2$ in $f_{5,n}$

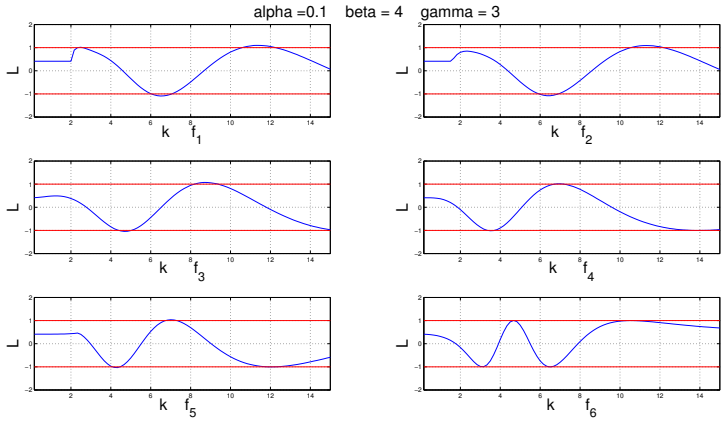

Fig. 1.2 Half the trace of the monodromy vs k. $\alpha = 0.1$, $\beta = 2$, $\gamma = 3$, $m = 1$, $h = 2$, $n = 2$ in $f_{5,n}$

that it does not necessarily brings instability, and that for larger k the behavior of L might be quite different, in particular for the last two functions.

In conclusion in all the numerical simulations we performed, at least for r_0 not too large, the evolution of L (linear stability) was very similar for values of k smaller than the slackening point r_0. Instabilities may occur for greater values of k but, of course, the last two models may behave quite differently.

Now we comment more accurately Fig. 1.3, showing for the function f_2 the behavior of the non-linear isoenergetic Poincaré map defined in section 1.2. The following simulations are calculated using the Matlab solver ode23t, keeping track of the decay of energy, which is about of 0.001% in sixty interactions.

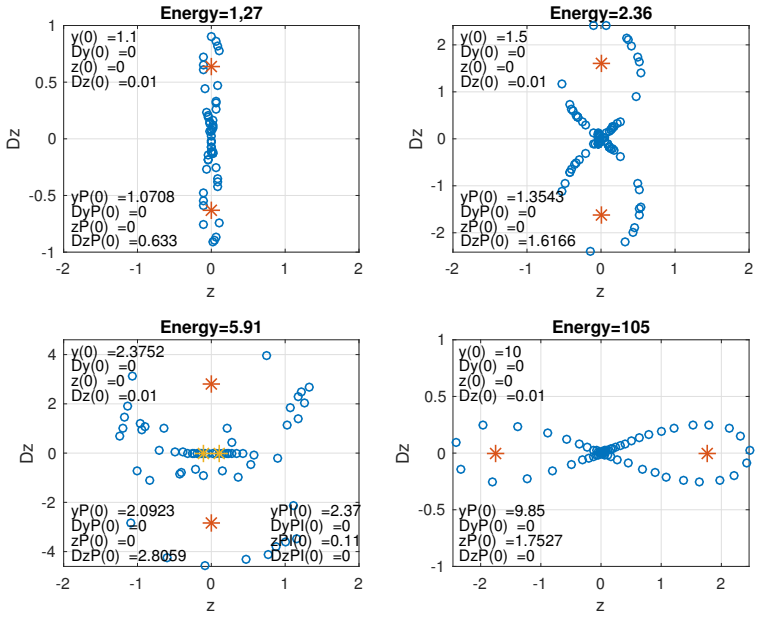

Fig. 1.3 Evolution of the nonlinear Poincaré map for function f_2, $\alpha = \beta = 0.1$, $\gamma = 3$, $m = h = 1$. In any subfigure (different levels of energy) the initial data for the interaction represented by blue circles can be found in the top left, the initial data for a periodic stable solution in the bottom left and the initial data for a periodic unstable solution in the bottom right

The study of the linearized map shows us that there are two intervals of instability, corresponding to approximately $1 < k < 2.5$ (that is energy $1 < E < 6$) and $5.5 < k < 12$ ($33 < E < 148$).

As L increases by crossing the lines $L = \pm 1$, two different types of bifurcations take place: two stable periodic points branch out of the origin with the same period of y when $L > 1$ and with doubled period when $L < -1$. In the case $L < -1$, towards the end of the first interval of instability, the stable periodic points stay approximately in the same place, while another couple of unstable periodic points with doubled period appear near the origin and collapse in the origin at the end of the interval of instability. In the case $L > 1$ it seems that there is only the couple of stable periodic points, that in the end collapses in the origin.

In Fig. 1.3 each blue small circle represents an interaction of the Poincaré map $\mathscr{P}_k$. The red stars correspond to stable periodic points, the yellow ones to unstable periodic points. The first three subfigures are related to the first interval of instability, the last one to the second. The evolution of the plot of the map in the second interval is indeed much simpler: the same pattern, from smaller to big, and again to small.

As a note, we choose to represent the Poincaré map $\mathscr{P}_k$, because of the nice "symmetry" with respect to the vertical axis.

The placing of the stable periodic points at the same level of energy has been computed using the twin Poincaré map $\mathscr{P}_{\mathscr{E}}$ where the manifold $\mathscr{E}(y,\dot{y},z,\dot{z}) = \mathscr{E}$ interesects the iperplane $y = 0$, under the condition $\dot{y} > 0$: the initial value problem for the Duffing equation (1.6) becomes

$$\ddot{w}_{\mathscr{E}}(t) + \alpha w_{\mathscr{E}}(t) + 2f(w_{\mathscr{E}}(t)) = 0, \qquad w_{\mathscr{E}}(0) = 0, \quad \dot{w}_{\mathscr{E}}(0) = \sqrt{2\mathscr{E}} > 0$$

and Proposition 1 has to be used in its more general form.

References

[AG] Arioli, G. and Gazzola, F. : A new mathematical explanation of what triggered the catastrophic torsional mode of the Tacoma Narrows Bridge. *Applied Mathematical Modelling*, **39**, 901–912 (2015).

[BFG] Benci, V. , Fortunato, D. and Gazzola, F. : Existence of torsional solitons in a beam model of suspension bridge *To appear*, 1–20 (2016).

[BG] Berchio, E. and Gazzola, F. : A qualitative explanation of the origin of torsional instability in suspension bridges. *Nonlinear Analysis*, **121**, 54–72 (2015).

[CW] Cazenave, T. and Weissler, F.B. : Unstable simple modes of the nonlinear string. *Quarterly of Applied Mathematics*, **54**, 287–305 (1996).

[Gaz] Gazzola, F. : *Mathematical Models for Suspension Bridges: Nonlinear Structural Instability*, MS&A. Modeling, Simulation and Applications, 15. Springer, Cham, (2015).

[GG] Ghisi, T. and Gobbino, M. : Unstable simple modes for a class of Kirchhoff equations. *Ann. Fac. Sci. Toulouse Math. (6)*, **10**, 639–658 (2001).

[MCKW] McKenna, P.J. and Walter, W. : Nonlinear oscillations in a suspension bridge. *Archive for Rational Mechanics and Analysis*, **98**, 167–177 (1987).

[MCKT] McKenna, P. J. and Tuama, C. Ó. : Large torsional oscillations in suspension bridges visited again: vertical forcing creates torsional response. *Amer. Math. Monthly* **108** (2001).

[Moo] Moore, K. S. : Large torsional oscillations in a suspension bridge: multiple periodic solutions to a nonlinear wave equation. *SIAM J. Math. Anal.*, **33**, 1411–1429 (2002).

[MP] Marchionna, C. and Panizzi, S. : An instability result in the theory of suspension bridges. *Nonlinear Analysis*, **140**, 12–28 (2016).